Chapter 3: Observations: Surface and Atmospheric Climate Change

Coordinating Lead Authors: Kevin E. Trenberth, Philip D. Jones

Lead Authors: Peter G. Ambenje, Roxana Bojariu, David R. Easterling, Albert M. G. Klein Tank, David E. Parker, James A. Renwick, Fatemeh Rahimzadeh, Matilde M. Rusticucci, Brian J. Soden, Pan-Mao Zhai

Contributing Authors: Robert Adler, Lisa Alexander, Hans Alexandersson, Richard P. Allan, Mark P. Baldwin, Martin Beniston, David H. Bromwich, Inés Camilloni, Christophe Cassou, Daniel R. Cayan, Edmund K. M. Chang, John R. Christy, Aiguo Dai, Clara Deser, Nikolai Dotzek, John Fasullo, Ryan L. Fogt, Christopher K. Folland, Piers Forster, Melissa Free, Christoph Frei, Byron Gleason, Jürgen Grieser, Pavel Y. Groisman, Sergey K. Gulev, James W. Hurrell, Masayoshi Ishii, Simon A. Josey, Per W. Kållberg, George N. Kiladis, Ramesh H. Kripalani, Kenneth E. Kunkel, Chiu Ying Lam, John R. Lanzante, Jay H. Lawrimore, David H. Levinson, Beate G. Liepert, Gareth J. Marshall, Carl A. Mears, Philip W. Mote, Hishashi Nakamura, Neville Nicholls, Joel R. Norris, Taikan Oki, Franklin R. Robertson, Karen H. Rosenlof, Fred H. Semazzi, Dennis J. Shea, J. Marshall Shepherd, Theodore G. Shepherd, Steven. C. Sherwood, Adrian J. Simmons, Ian Simmonds, Peter C. Siegmund, Chris D. Thorncroft, Peter W. Thorne, Sakari M. Uppala, Russell S. Vose, Bin Wang, Stephen G. Warren, Richard Washington, Matthew C. Wheeler, Bruce A. Wielicki, Takmeng Wong, David B.Wuertz.

Review Editors: Brian J. Hoskins, Bubu P. Jallow, Thomas R. Karl

Date of Draft: 22 February 2006:

Notes: This is the TSU compiled version. All figures are designed for single column presentation (e.g., Figures. 3.2.1, 3.2.9, 3.4.3, 3.4.5, etc.) or full page width (e.g., Figures 3.2.10, Question 3.1, Figure 1). The latter applies for panels aligned side by side (e.g., Figures 3.2.4, 3.2.5) and for the major assemblages Figures 3.3.3 and 3.8.3. Figure 3.3.3 will appear sideways, as given here. Otherwise, the figures should fit in a single column.

Figures

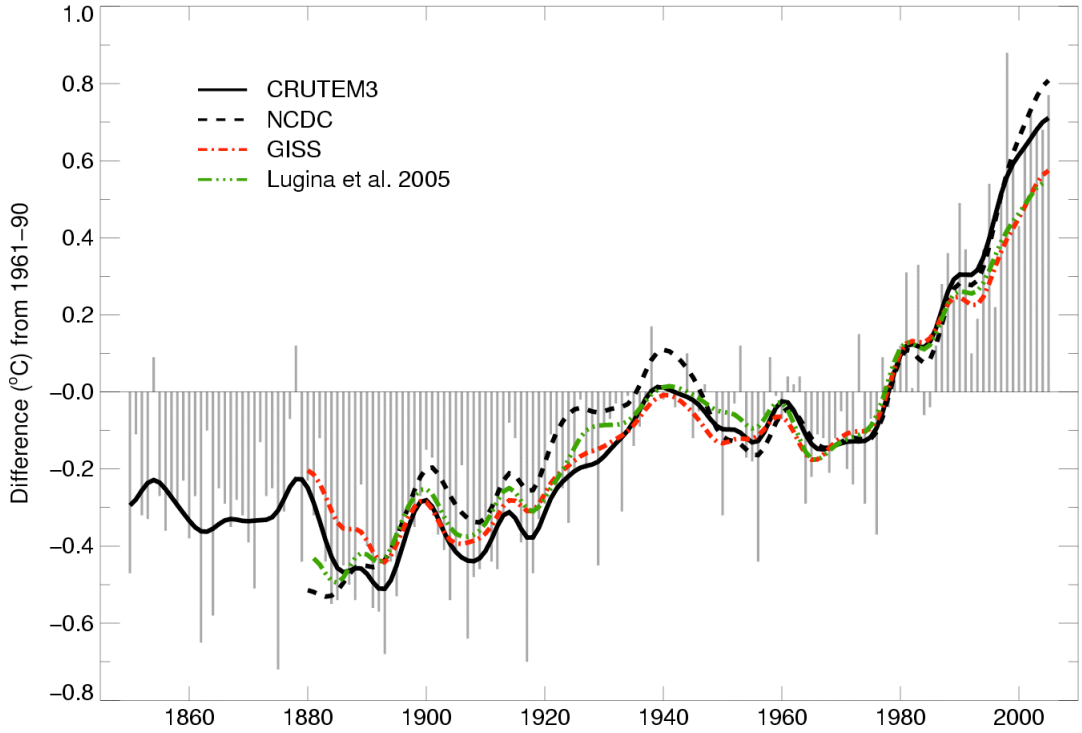

Figure 3.2.1. Annual anomalies of global land surface air temperature, 1861 to 2005, relative to the 1961–1990 mean (°C) for CRUTEM3 updated from Brohan et al. (2006). The smooth curves depict decadal variations (see Appendix 3.A). The thick solid black curve from CRUTEM3 is compared with those from NCDC (Smith and Reynolds, 2005) (black dashed) and GISS (Hansen et al., 2001) (red dashed) and Lugina et al. (2005) (green dashed).

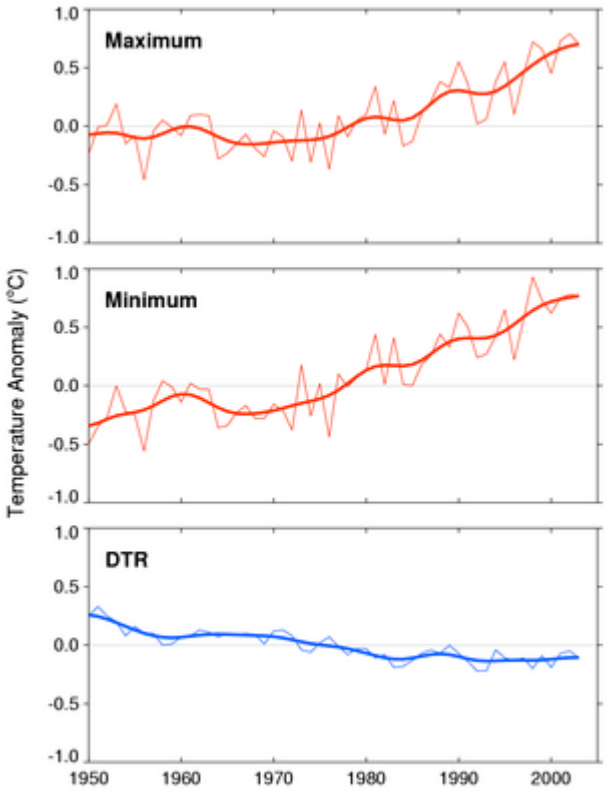

Figure 3.2.2. Annual anomalies relative to the 1961–1990 mean of maximum and minimum temperatures and diurnal temperature range (°C) averaged for the 71% of global land areas where data are available for 1950 to 2004. The smoothed curve shows the decadal variability (Appendix 3.A). Adapted from Vose et al. (2005a).

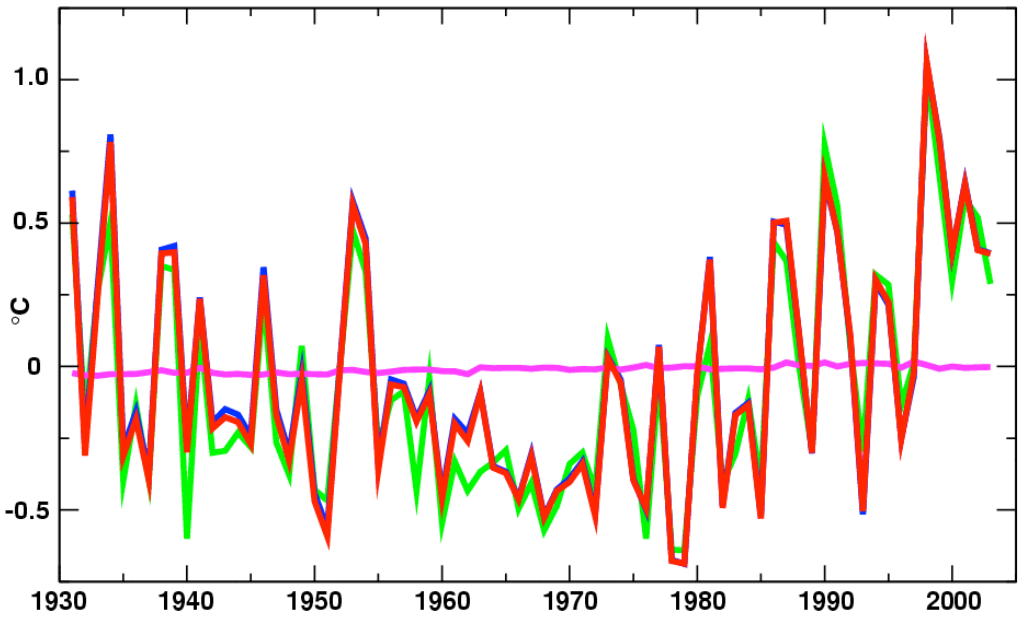

Figure 3.2.3. Anomaly (°C) time series relative to the 1961-90 mean of the full USHCN data (red), the USHCN data without the 16% of the stations with populations of over 30,000 within 6 km in the year 2000 (blue), and the 16% of the stations with populations over 30,000 (green). The full USHCN set minus the set without the most urban stations is shown in magenta. Both the full data set and the data set without the high population stations had stations in all of the 2.5° latitude by 3.5° longitude grid boxes during the entire period plotted but the subset of high population stations only had data in 56% of these grid boxes.

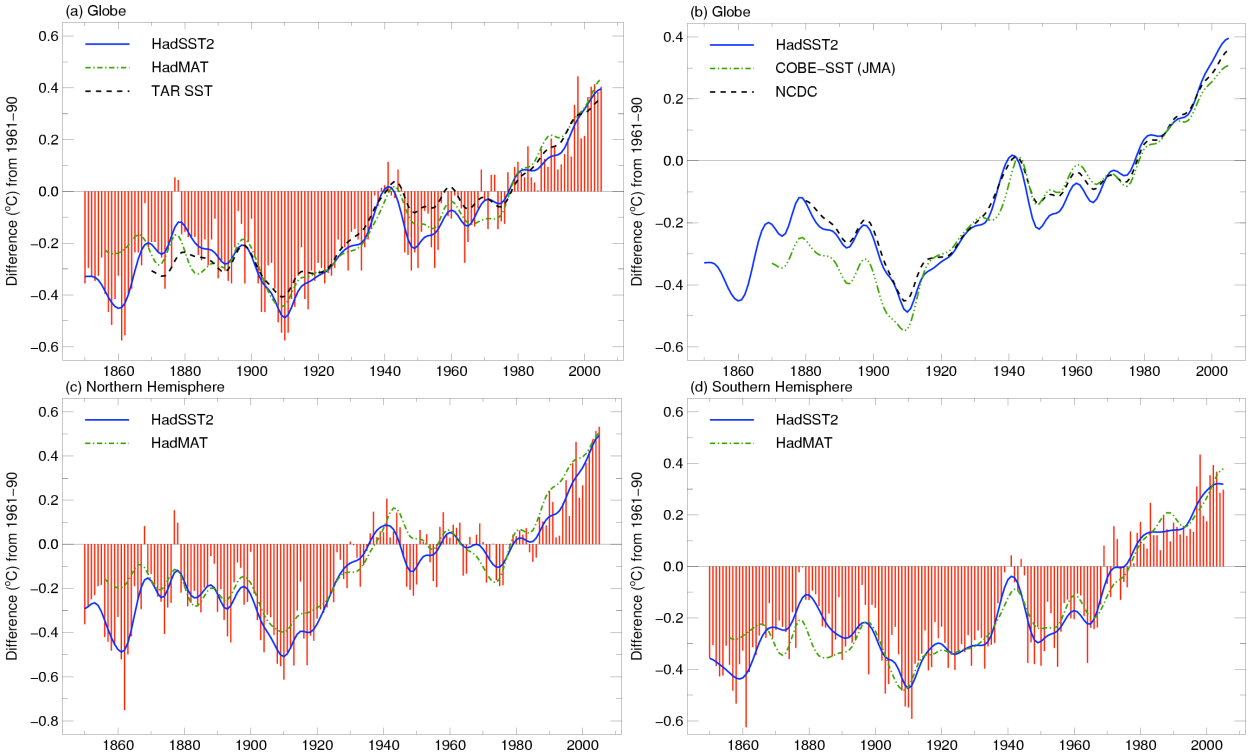

Figure 3.2.4. (a) Annual anomalies of global SST (HadSST2; red bars and blue solid curve) and global night marine air temperature (HadMAT, dotted green curve), 1850 to 2005, relative to the 1961–1990 mean (°C) from UKMO (Rayner et al., 2006). The decadal filter (Appendix 3.A) provides the smoothed curves. The dashed black curve shows equivalent smoothed SST anomalies from the TAR. (b) Smoothed annual global SST 1850 to 2005, relative to 1961–1990 (°C), from HadSST2 (thick blue line as in a) and from Reynolds et al. (2002) (NCDC; dashed black line, includes satellite data), and from Japan [(Ishii et al., 2005) COBE-SST (JMA)], green dashed line. These latter two series and HadMAT begin later in the 19th century than HadSST2. (c, d) as in (a) but for the NH and SH showing only the UKMO (Rayner et al., 2006) series.

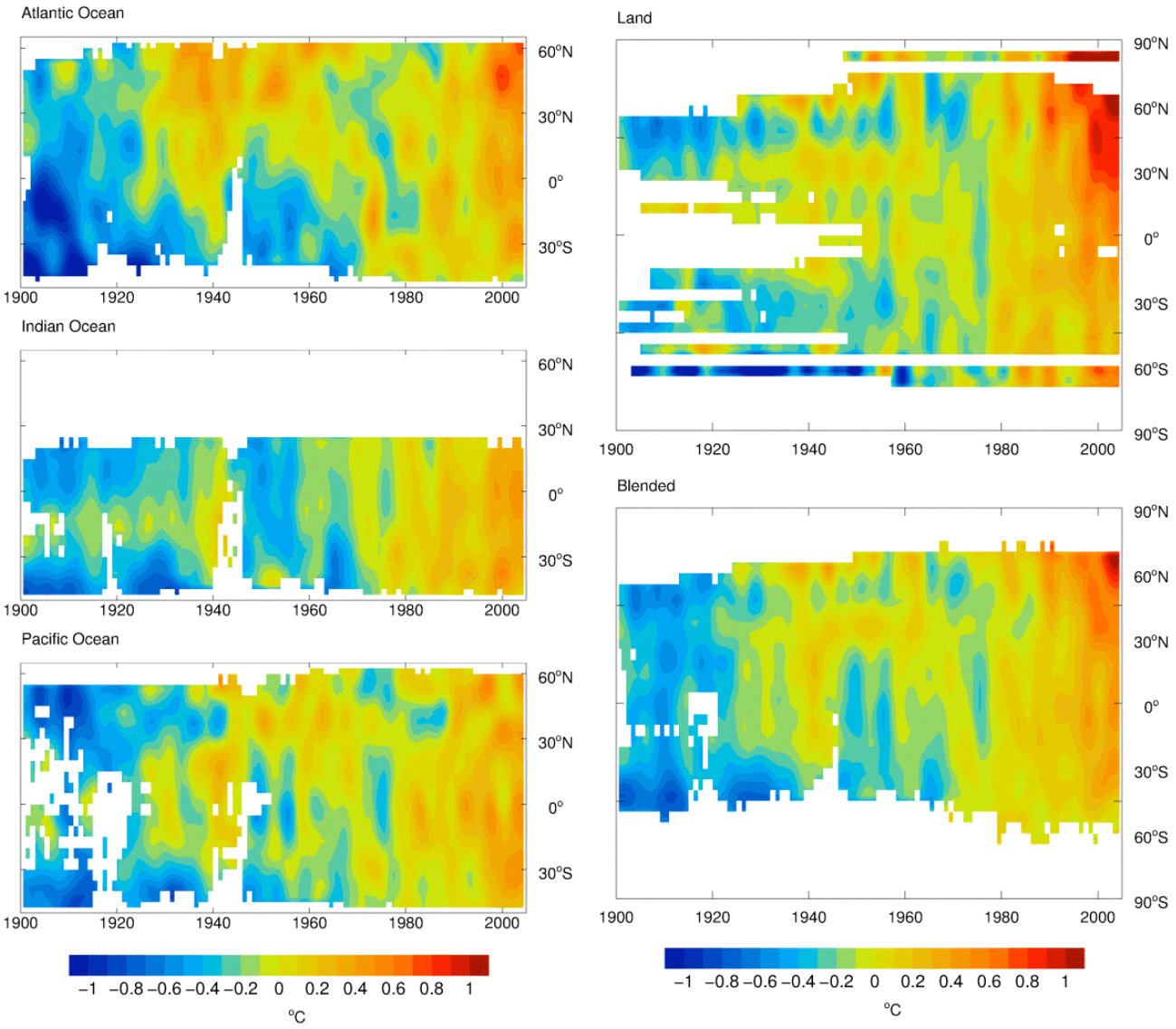

Figure 3.2.5. Latitude-time sections of zonal mean temperature from 1900 to 2005, relative to the 1961–1990 mean (°C). Left panels: SST annual anomalies across each ocean from HadSST2 (Rayner et al., 2006). Right panels: Surface temperature annual anomalies for land (top, CRUTEM3) and land plus ocean (bottom, HadCRUT3). The values are smoothed with a 1/12(1–3–4–3–1) filter to remove fluctuations less than 6 years or so (see Appendix 3.A) and missing data are white.

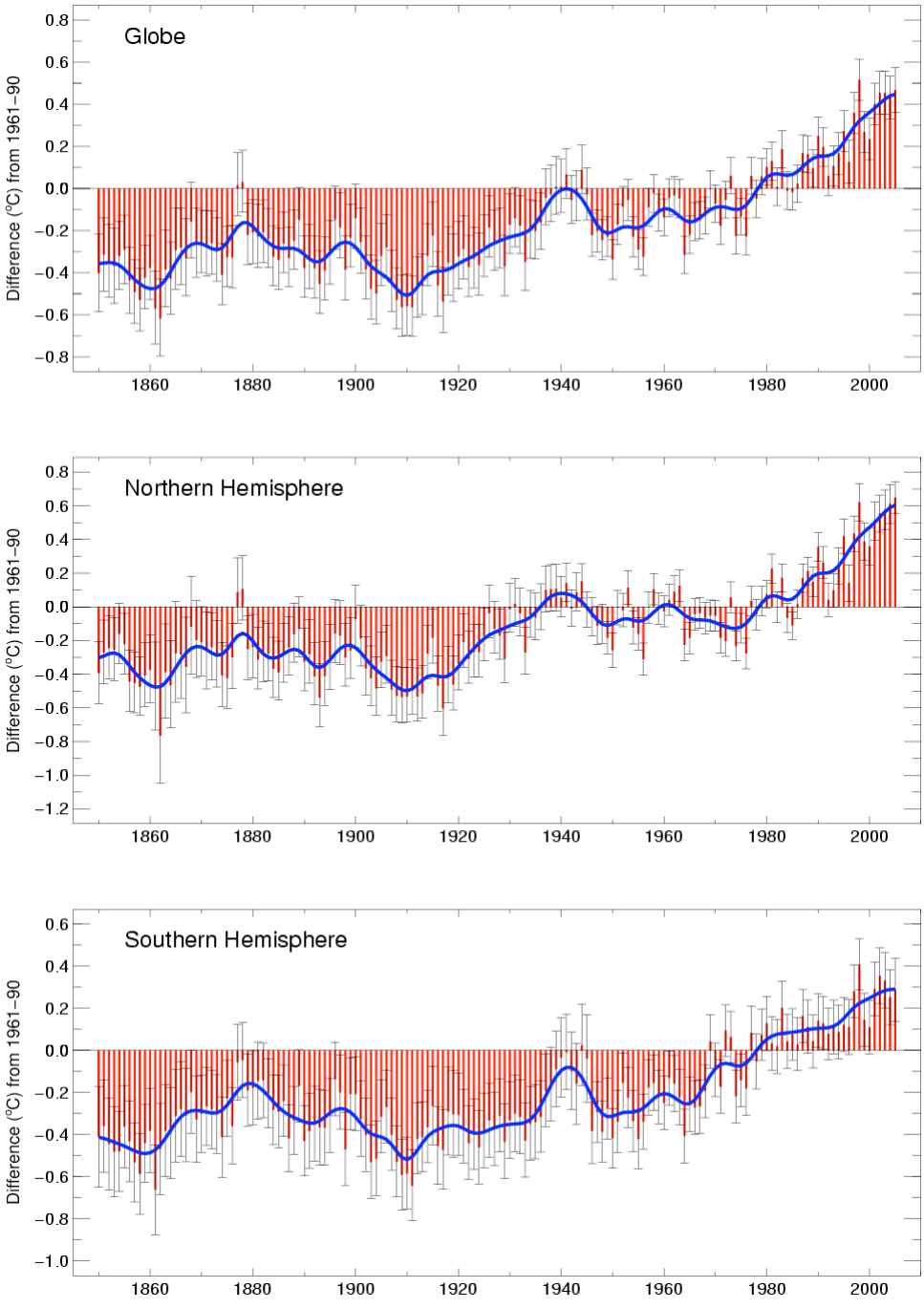

Figure 3.2.6. Global and hemispheric annual combined land surface air temperature and SST (°C) (red) relative to the 1961–1990 mean, along with ±2 standard error ranges, from HadCRUT3 (Brohan et al., 2006). The blue decadal smoothing is described in Appendix 3.A.

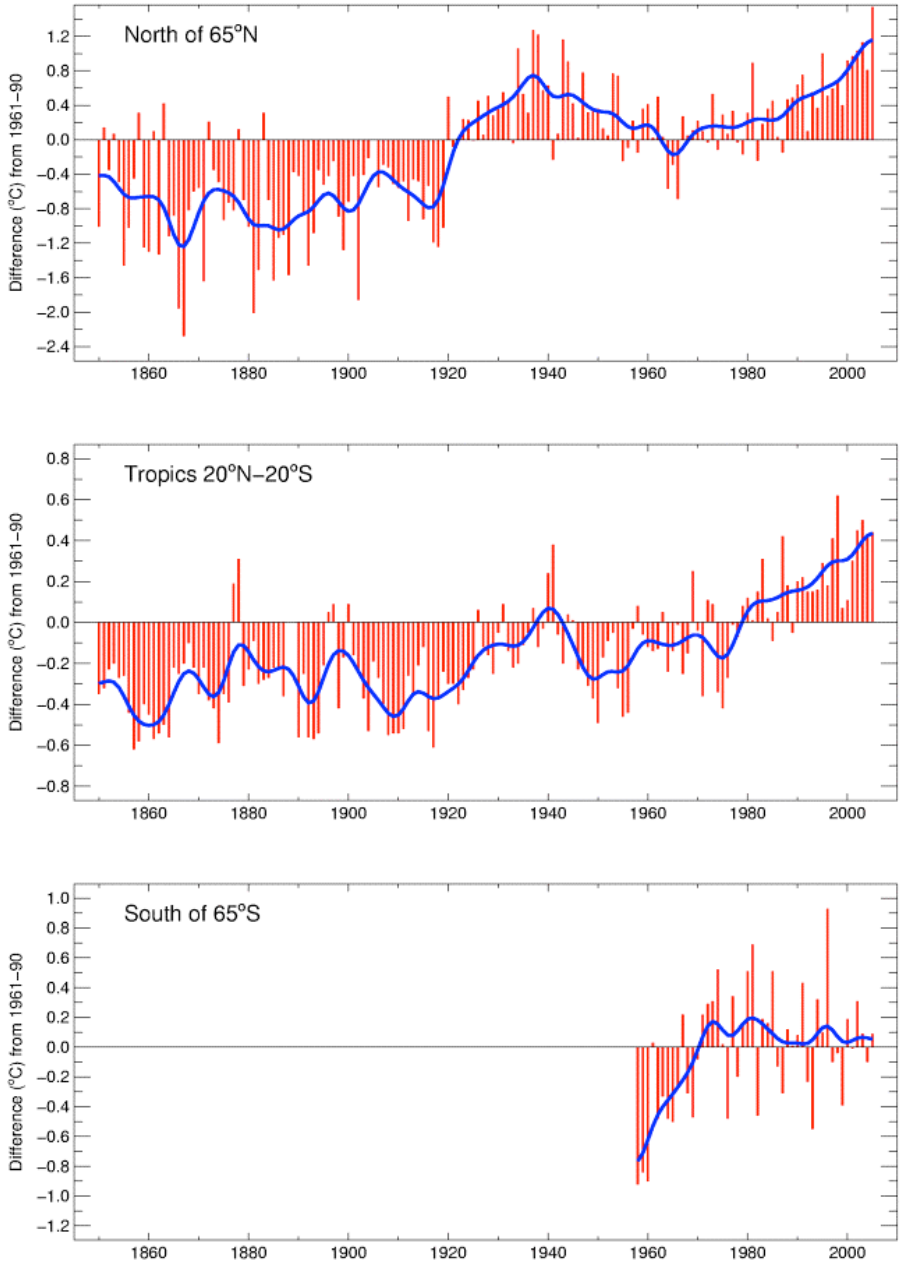

Figure 3.2.7. Annual combined land surface air temperature and SST (°C), relative to the 1961–1990 mean, from HADCRUT3 (Brohan et al., 2006) for the tropics (20°N–20°S), and polar regions north and south of 65°. Blue decadal smoothing is described in Appendix 3.A.

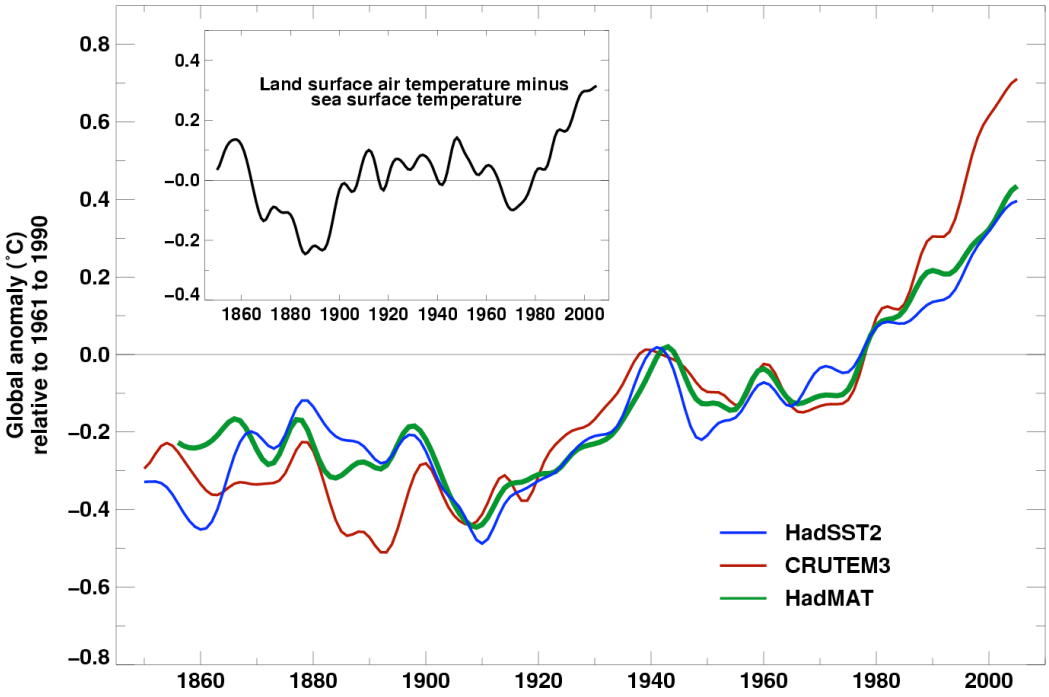

Figure 3.2.8. Smoothed annual anomalies of global average sea surface temperature (blue curve), night marine air temperature (green curve) and land surface air temperature (red curve) 1861 to 2005, relative to their 1961–1990 means (°C) (Rayner et al., 2006; Brohan et al., 2006). Also shown (inset) are the smoothed differences between the land-surface air and SST anomalies (i.e., red minus blue).

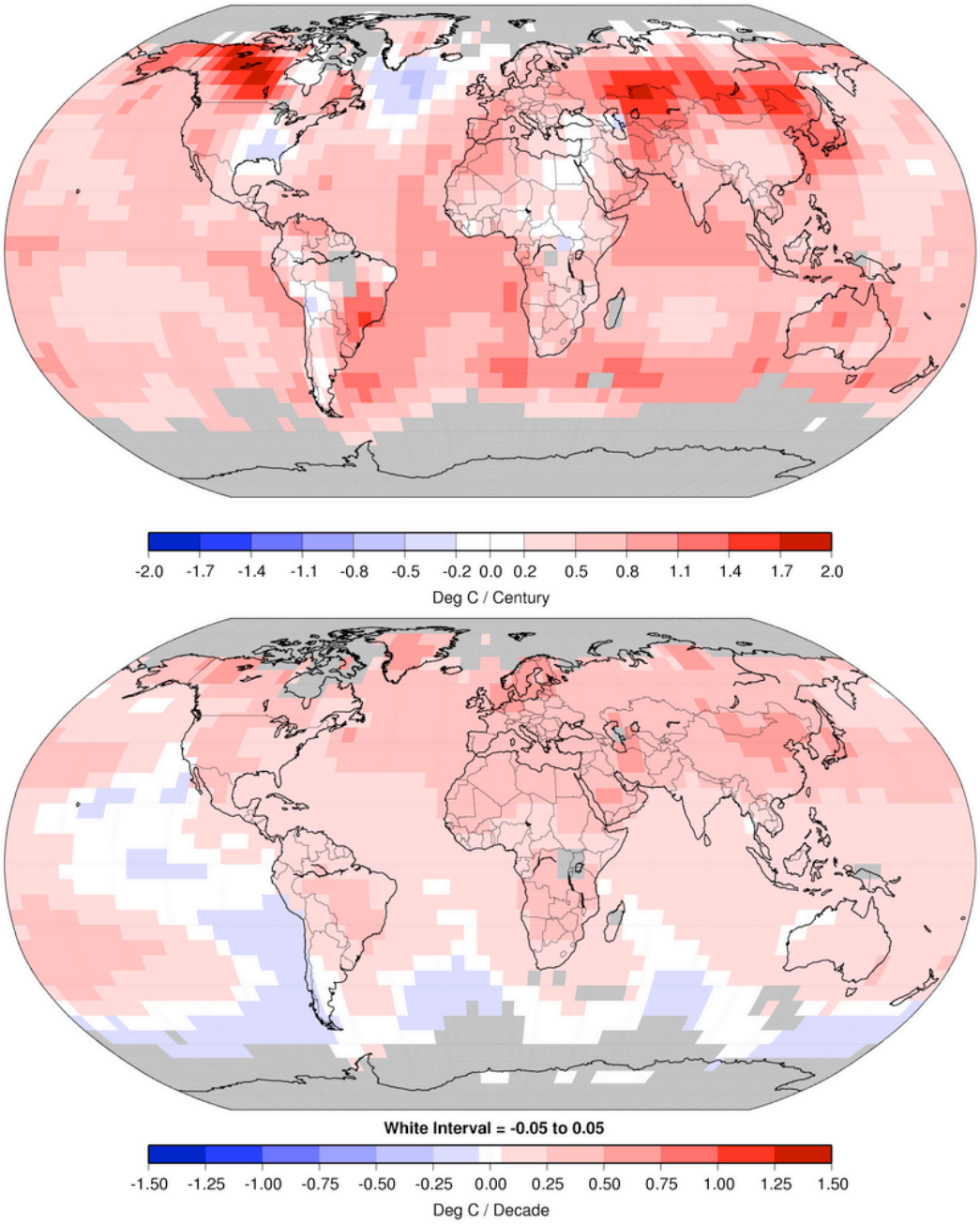

Figure 3.2.9. Linear trend of annual temperatures for 1901–2005 (upper; °C century^{-1}) and 1979–2005 (lower; °C decade^{-1}). Areas in grey have insufficient data to produce reliable trends. The minimum number of years needed to calculate a trend value is 66 years for 1901–2005 period and 18 years for 1979–2005. An annual value is available if there are 10 valid monthly temperature anomaly values. The dataset used was produced by NCDC from Smith and Reynolds (2005).

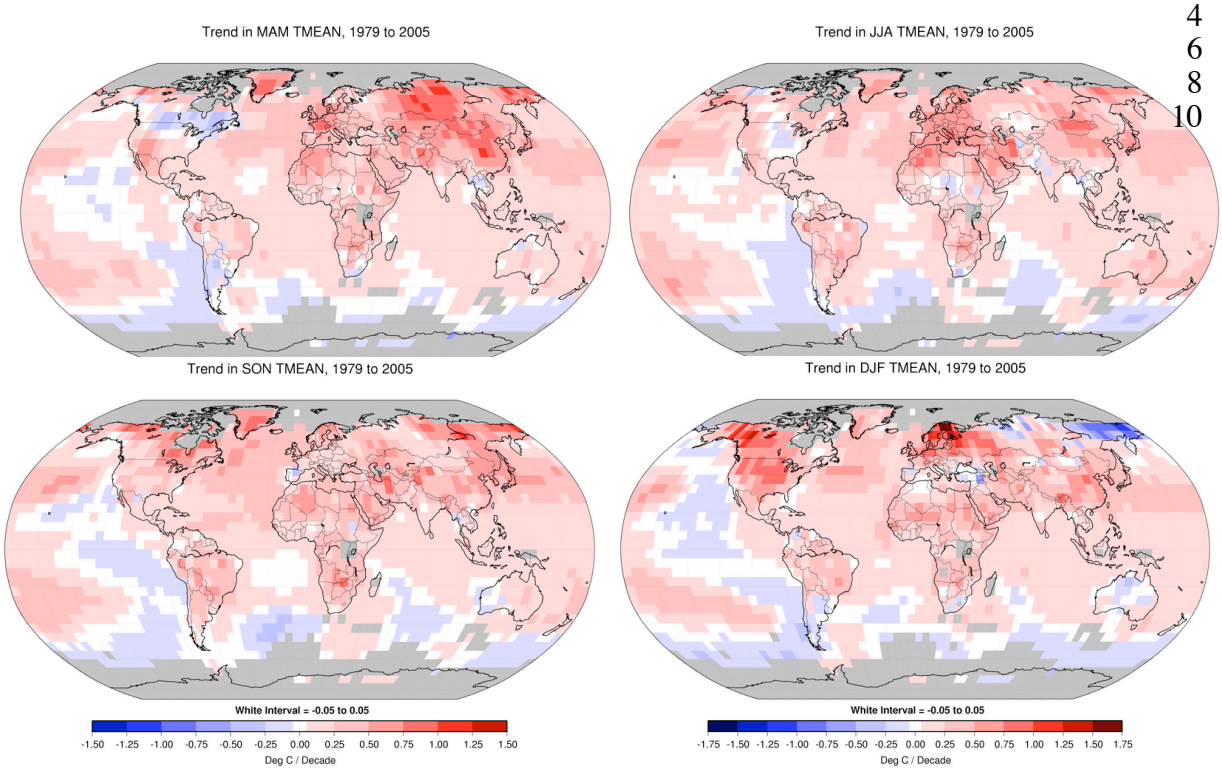

Figure 3.2.10. Linear trend of seasonal MAM, JJA, SON and DJF temperature for 1979–2005. The units are °C decade^{-1}. Areas in grey have insufficient data to produce reliable trends. The minimum number of years to calculate a trend value is 18. A seasonal value is available if there are 2 valid monthly temperature anomaly values. The dataset used was produced by NCDC from Smith and Reynolds (2005).

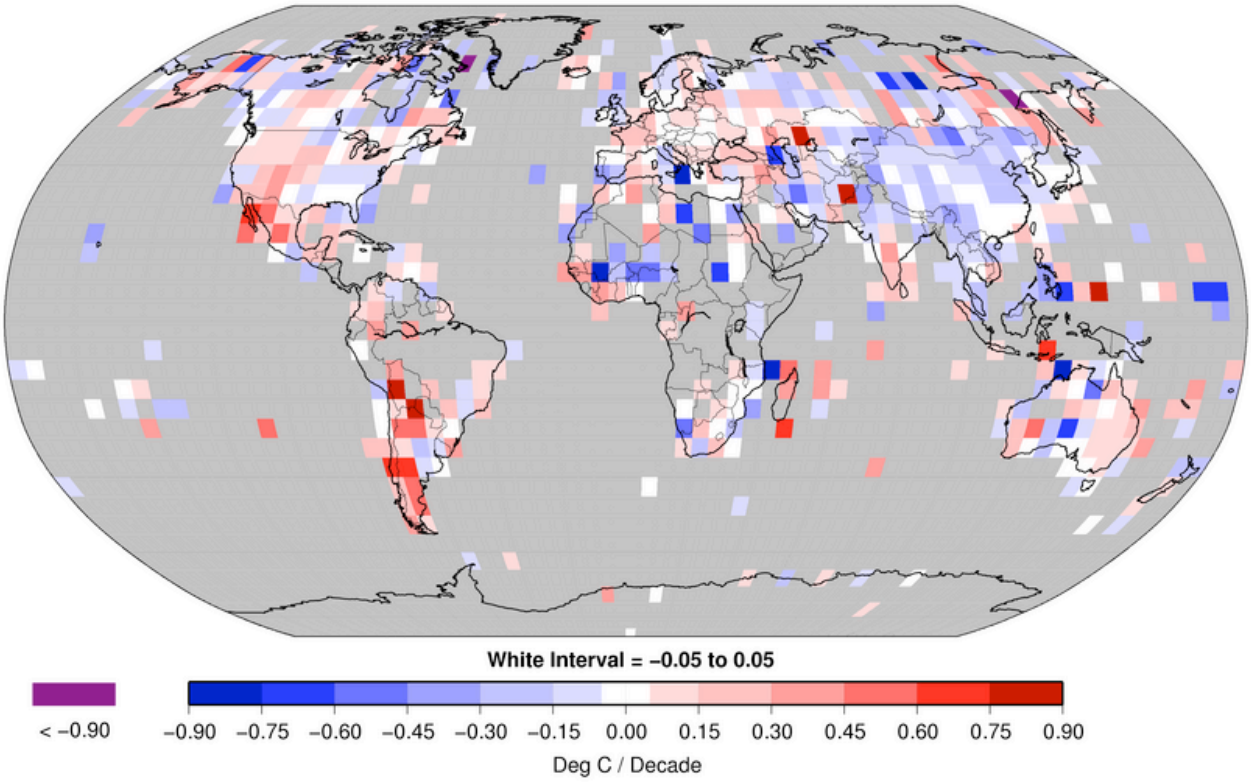

Figure 3.2.11. Linear trend in annual mean DTR for 1979 to 2004 in °C decade^{-1}. Grey regions indicate incomplete or missing data. After Vose et al. (2005a).

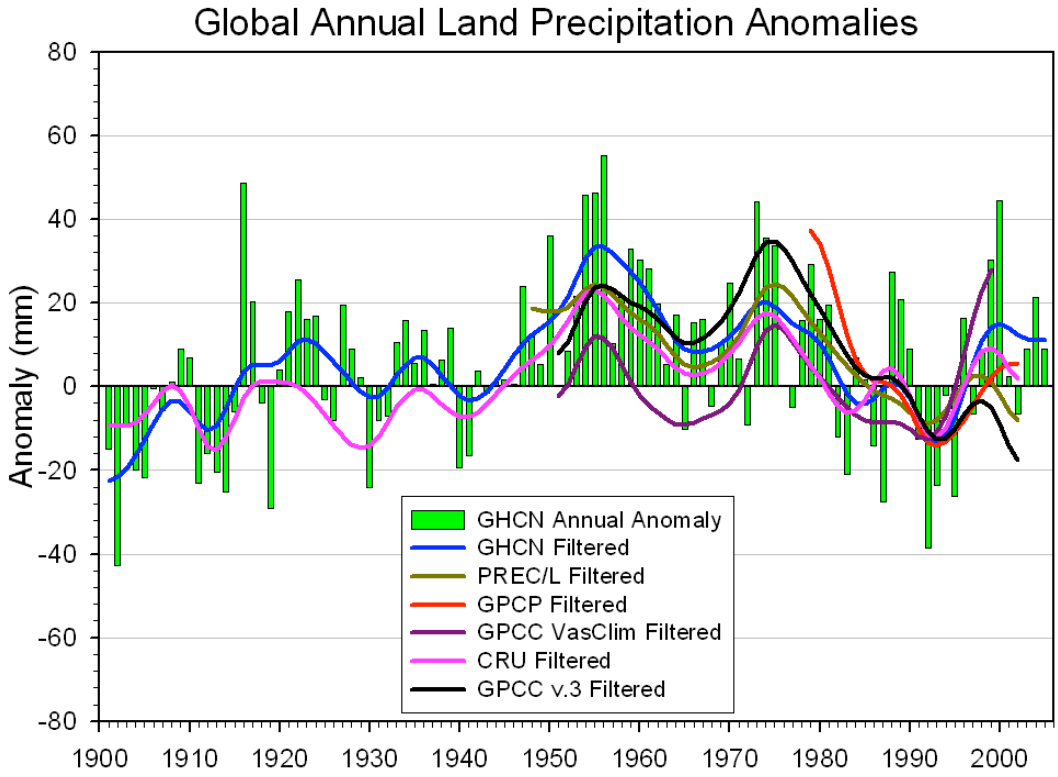

Figure 3.3.1. Time series for 1900 to 2005 of annual global land precipitation anomalies from GHCN with respect to the 1981–2000 base period (to convert to mm/day divide by 365 or 366). Smoothed values (using the decadal filter in Appendix 3.A) are also given for the GHCN (Peterson and Vose, 1997), PREC/L (Chen et al. (2002)), GPCP (Adler et al., 2003), GPCC (Rudolf et al., 1994) and CRU (Mitchell and Jones, 2005).

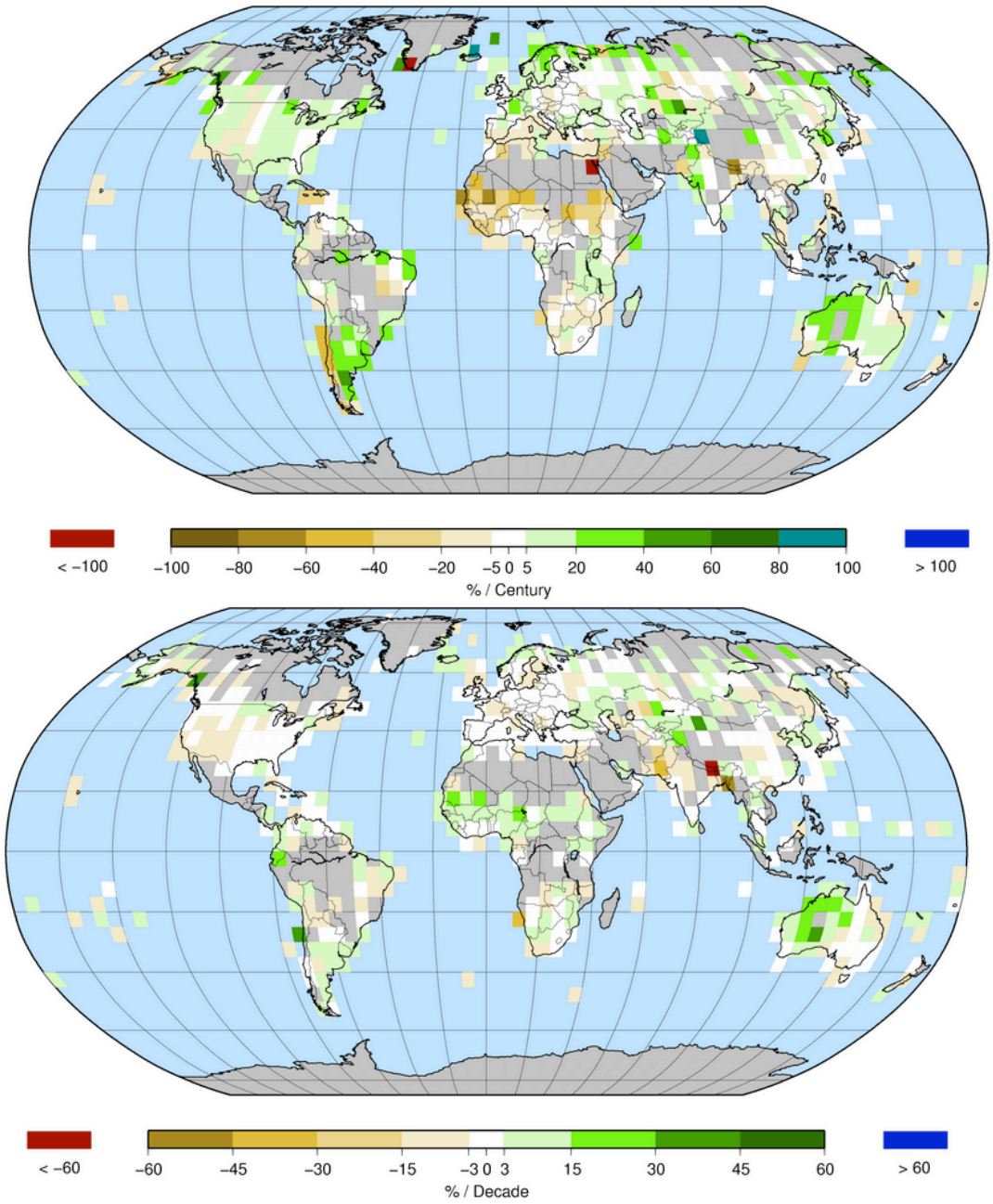

Figure 3.3.2. Trend of annual precipitation amounts for 1901–2005 (upper, % century^{-1}) and 1979–2005 (lower, % decade^{-1}) the percentage being based on the 1961-90 period. Areas in grey have insufficient data to produce reliable trends. The minimum number of years to calculate a trend value is 66 for 1901–2005 period and 18 for 1979–2005. An annual value is complete for a given year if all twelve monthly percentage anomaly values are present. The GHCN precipitation dataset from NCDC was used.

.